

An Adapter-free Fine-tuning Approach for Tuning 3D Foundation Models

Sneha Paul^[0000-0001-7731-4196], Zachary Patterson^[0000-0001-8878-7845], and
Nizar Bouguila^[0000-0001-7224-7940]

Concordia University, Montreal, Canada

Abstract. Point cloud foundation models demonstrate strong generalization, yet adapting them to downstream tasks remains challenging in low-data regimes. Full fine-tuning often leads to overfitting and significant drift from pre-trained representations, while existing parameter-efficient fine-tuning (PEFT) methods mitigate this issue by introducing additional trainable components at the cost of increased inference-time latency. We propose **Momentum-Consistency Fine-Tuning (MCFT)**, an adapter-free approach that bridges the gap between full and parameter-efficient fine-tuning. MCFT selectively fine-tunes a portion of the pre-trained encoder while enforcing a momentum-based consistency constraint to preserve task-agnostic representations. Unlike PEFT methods, MCFT introduces no additional representation learning parameters beyond a standard task head, maintaining the original model’s parameter count and inference efficiency. We further extend MCFT with two variants: a semi-supervised framework that leverages abundant unlabeled data to enhance few-shot performance, and a pruning-based variant that improves computational efficiency through structured layer removal. Extensive experiments on object recognition and part segmentation benchmarks demonstrate that MCFT consistently outperforms prior methods, achieving a 3.30% gain in 5-shot settings and up to a 6.13% improvement with semi-supervised learning, while remaining well-suited for resource-constrained deployment.

Keywords: Representation learning · transfer learning · point cloud · semi-supervised learning · pruning

1 Introduction

The recent rise of foundation models has showcased remarkable generalization capabilities and human-like performance across a range of domains. These models, pre-trained on large-scale datasets to learn general-purpose representations, have become essential tools in areas such as 2D computer vision and natural language processing (NLP). A similar trend is observed in point clouds, an unstructured 3D geometric data that plays a crucial role in real-world applications by enabling accurate object recognition and scene understanding in complex 3D environments. Foundation models for point clouds have shown promising performance and generalization capabilities [19, 33]. However, to fully leverage their

potential for specific downstream tasks, additional fine-tuning is still required [30, 5].

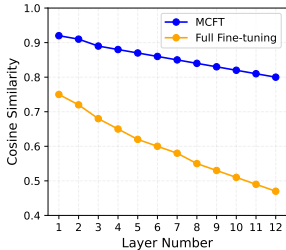


Fig. 1: Layer-wise similarity

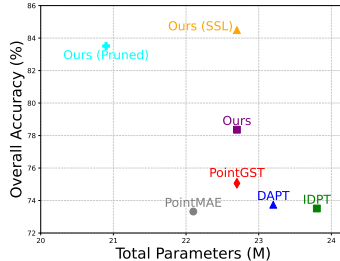


Fig. 2: Parameters vs performance

Fine-tuning a foundation model for downstream tasks presents significant challenges, particularly when training data is limited. Tuning with scarce data often leads to overfitting and a loss of generalization, diminishing the foundation model’s effectiveness. For instance, as illustrated in Fig 1, full fine-tuning (FFT) leads to overfitting and significant divergence from the pre-trained model’s representations, particularly in deeper layers. In 2D vision and NLP domains, recent studies [9, 13, 2] have explored various Parameter-Efficient Fine-Tuning (PEFT) techniques to address this issue. These methods have achieved state-of-the-art (SOTA) performance by introducing additional trainable parameters, such as adapters [2] or prompts [23], while keeping the pre-trained model weights frozen. Inspired by this, PEFT techniques have been adopted to 3D as well [35, 45, 16]. However, unlike other domains, PEFT methods for 3D foundation models show only a minimal performance gain when applied in a low-data scenario (order of 1% improvement), as illustrated in Fig 2. Furthermore, PEFT introduces additional trainable parameters to the frozen encoder, which increase the overall memory and compute cost of the model *during inference* — a bottleneck for deploying such a model in a resource-constrained environment like mobile devices. For instance, IDPT [35] introduces 1.7 million extra parameters to the pre-trained PointMAE encoder (Fig 1), which results in a staggering 50% increase in inference latency (see Table 3 for more details).

To address these challenges, we propose Momentum-Consistency Fine-Tuning (MCFT), an adapter-free approach that bridges the gap between FFT and PEFT for fine-tuning 3D foundation models in low-data settings. Unlike PEFT methods that insert adapter modules or prompts into the frozen encoder for adaptation, MCFT does not introduce any additional parameters for tuning the encoder—except a standard task-specific prediction head (e.g. classifier layer). The core idea of MCFT is a selective fine-tuning approach of a defined portion of the pre-trained encoder by enforcing our proposed consistency constant to avoid overfitting. This approach matches the original model’s parameter count and computational efficiency without the additional representation learning parameters introduced by PEFT methods. As illustrated in Fig 2, MCFT maintains

a high degree of similarity to the pre-trained encoder across layers, in contrast to FFT, which increasingly diverges, particularly in deeper layers, resulting in diminished generalization.

Additionally, we introduce two variants of MCFT to further improve performance and efficiency in few-shot scenarios. The first is a *semi-supervised* momentum-consistency fine-tuning framework that leverages unlabelled data (which are easy and abundant to collect) alongside limited labelled data. Specifically, we adopt the semi-supervised learning protocol from AllMatch [20] in conjunction with our MCFT regularization to effectively utilize the unlabelled data. The second variant is a lighter version of MCFT that focuses on enhancing computational efficiency through structural pruning. While MCFT already maintains the efficiency of the pre-trained encoder, this variant selectively prunes less important layers, producing a smaller and faster model without significantly compromising performance.

We evaluate MCFT extensively on object recognition in n -way few-shot [39], full few-shot, and fully-supervised setups using synthetic [40] and real-world [28] datasets, as well as part-segmentation tasks on ShapeNetPart [32]. Along with n -way (5 and 10-way) few-shot setups, we also report a full few-shot evaluation by testing performance across all dataset classes. This protocol is significantly more challenging than n -way evaluation as the model must learn to distinguish among all classes simultaneously rather than a small subset. Our results show that MCFT consistently outperforms existing approaches in all settings. Notably, in the 5-shot evaluation, MCFT achieves a **3.30%** improvement over prior methods, demonstrating its robustness in low-data scenarios. Furthermore, our semi-supervised variant yields an additional **6.13%** increase over the standard few-shot results. Finally, our pruned variant maintains comparable performance to the full model while reducing computational overhead, making it ideal for resource-constrained environments.

2 Related Work

PEFT in Point Clouds. Parameter-Efficient Fine-Tuning (PEFT) reduces adaptation cost by updating a small subset of parameters while keeping the backbone frozen. Common PEFT paradigms include prompt-based methods, which introduce learnable tokens into the input or attention space [12, 13], and adapter-based methods, which insert lightweight trainable modules into the network [2]. Low-rank re-parameterization further improves efficiency by decomposing weight updates into compact subspaces [9]. Recent extensions explore structural re-parameterization and task-specific token aggregation to better integrate task knowledge into frozen backbones [17, 24]. PEFT for 3D point clouds is relatively underexplored. IDPT [35] first introduced instance-aware prompts for point cloud backbones, while DAPT [45] combined dynamic adapters with prompt tuning. PPT [38] proposed trainable positional embeddings derived from sampled and clustered tokens. PointPEFT [27] integrates lightweight adapters with input-level prompts, achieving competitive performance with limited pa-

parameter overhead. However, existing methods uniformly introduce additional trainable parameters, increasing memory and training cost, which limits their suitability for deployment on resource-constrained devices.

Semi-supervised Learning in Point Clouds. Semi-supervised learning (SSL) for point clouds aims to reduce reliance on labeled data. Prior work primarily focuses on enforcing prediction consistency across augmented point clouds [1] or aligning features with class-level prototypes in multi-modal settings [3]. To mitigate class imbalance, ConFid [4] resamples unlabeled data based on class-wise confidence, while AllMatch [20] maximizes utilization of the unlabeled set through unified matching strategies. Despite these advances, SSL has not been studied in the context of adapting large 3D foundation models.

Pruning for Model Compression. Pruning improves model efficiency by removing parameters with low importance. Unstructured pruning achieves high sparsity but often requires specialized hardware [25], whereas structured pruning removes entire blocks or layers, yielding predictable acceleration [11]. Pruning is commonly applied after fine-tuning, making it compatible with PEFT pipelines. Recent methods combine pruning with low-rank adaptation or task-aware compression. SPA [7] integrates structured pruning with compact adapters, while CPET [44] combines pruning, low-rank tuning, and distillation. Other approaches jointly prune and adapt parameters but rely on static tuning configurations [37, 14]. APT [42] addresses this limitation via dynamic salience-based tuning and pruning. However, pruning has not yet been explored for efficient adaptation of 3D foundation models.

3 MCFT: Momentum-Consistency Fine-Tuning

Transformers have become an effective architecture for processing 3D point clouds due to their ability to capture complex spatial relationships [19]. In a typical point cloud model, such as Point-MAE [19], a raw point cloud $X \in \mathbb{R}^{M \times 3}$, containing M points, is segmented into smaller patches $X' \in \mathbb{R}^{m \times k \times 3}$ using Farthest Point Sampling (FPS) and K-Nearest Neighbour (KNN) algorithms. Here, m denotes the number of patches, and each patch contains k local points. These patches are transformed into input tokens, represented as $E_0 \in \mathbb{R}^{m \times d}$, where d is the embedding dimension. To incorporate positional information, the patches are further embedded using a point patch embedding module. Additionally, a classification token ([CLS]) is added to the sequence of input tokens. The combined sequence passes through a series of transformer layers, each consisting of self-attention and feed-forward modules, which are responsible for learning meaningful representations. Such an encoder, when pre-trained on large unlabelled data, learns generalizable features of a particular domain. Once pre-trained, the encoder can be fine-tuned with minimal supervision to perform any downstream task. However, fine-tuning a foundation model with limited labelled data is challenging, primarily due to the massive size of the model, which can easily lead to overfitting. To deal with such issues, PEFT incorporates additional learnable parameters into the frozen pre-trained model. While such a concept shows desir-

able performance improvement, it increases the number of parameters and the inference cost of the model. In this work, we focus on fine-tuning a foundation model to improve its performance on the downstream task without increasing its inference cost.

We propose Momentum-Consistency Fine-tuning (MCFT), an adapter-free tuning approach for tuning a foundation model without introducing any additional parameters **into the pre-trained encoder** to maintain the efficiency of the pre-trained encoder. Only a task-specific prediction layer (e.g. a classifier head) is added on top of the encoder to generate the prediction (e.g. class distribution), which is not specific to our method and is required to generate the prediction. The core idea of our proposed solution is to strategically fine-tune a few layers of the pre-trained encoder with a novel momentum-consistency-based self-distillation module that regularizes the learning process by aligning the embeddings of the trainable model (student) with those of the pre-trained model (teacher). We enable learning the new concept by fine-tuning a few layers of the pre-trained encoder; at the same time, the self-distillation concept ensures that the fine-tuning does not overfit the new small data and lose its generalization. However, a naive self-distillation (without our momentum update concept) with the pre-trained model restricts the learning to the knowledge of the pre-trained encoder. To alleviate this limitation, we slowly update the pre-trained encoder as the exponential moving average (EMA) of the learnable encoder. This provides a stable regularization target that prevents the learnable encoder from overfitting to limited training data.

Formally, let $E_s \in \mathbb{R}^d$ denote the [CLS] embedding from the student model and $E_t \in \mathbb{R}^d$ be the [CLS] embedding from the teacher model. The alignment loss is defined with a cosine distance loss function as:

$$\mathcal{L}_{\text{align}} = 1 - \frac{E_s^T \cdot E_t}{\|E_s\| \|E_t\|}, \quad (1)$$

where $\mathcal{L}_{\text{align}}$ measures the cosine similarity between the [CLS] embeddings, promoting consistency across models. This alignment mitigates overfitting and ensures better generalization on downstream tasks.

In addition, we *add a classifier head* that takes the embedding E_s and generates class predictions, y_i . This classifier head enables the model to directly learn task-specific features and improves classification performance. To train the classifier, we use a cross-entropy loss defined as follows:

$$\mathcal{L}_{\text{sup}} = - \sum_{i=1}^C y_i \log(\hat{y}_i), \quad (2)$$

where C is the number of classes, y_i is the ground-truth label, and \hat{y}_i is the predicted probability for class i . Initially, the classifier head is trained along with the feature encoder for a fixed number of epochs. Then, we follow the full fine-tuning protocol where the parameters of the momentum encoder are updated using the EMA approach. Let, θ_s and θ_t represent the parameters of the online and momentum encoders, the EMA update is defined as $\theta_t = \alpha \cdot \theta_t + (1 - \alpha) \cdot \theta_s$, where $\alpha \in [0, 1]$ is the smoothing factor controlling the contribution of the previous

Table 1: Comparison of the object recognition task on the ModelNet40 and ScanObjectNN (OBJ_ONLY) dataset in *full* few-shot setup.

Methods	ModelNet40			ScanObjectNN		
	5-shot	10-shot	20-shot	5-shot	10-shot	20-shot
Point-BERT [33]	72.88±2.3	79.31± 2.1	82.11±2.7	56.92±1.8	64.84±1.9	74.13±2.4
+ IDPT [35]	73.97 ±1.8	80.58± 1.9	84.43±1.7	57.23±2.1	65.88±2.5	75.11±2.3
+ DAPT [45]	73.68± 1.3	80.47±1.9	83.87±2.2	57.89±2.5	66.03±1.7	75.12±2.9
+ PointGST [16]	75.14±1.6	81.25±2.3	85.17±1.9	59.35±1.9	66.14±1.8	76.08± 2.1
+ MCFT	77.91±2.3	82.93±1.2	86.68±1.7	60.97±1.2	67.23±1.5	76.78±2.1
Point-MAE [19]	73.32±2.1	79.97± 2.5	83.78±1.7	56.37±1.2	65.39±1.8	74.86±2.2
+ IDPT [35]	73.51 ±2.8	80.24± 1.7	83.91±1.6	57.01±2.2	65.88±2.5	75.58±2.7
+ DAPT [45]	73.74±1.6	80.83±2.1	84.40±1.9	57.21±2.2	66.25±2.6	75.81±2.1
+ PointGST [16]	75.06±1.9	81.02±2.9	84.91±2.7	58.23±1.8	66.75±2.2	76.18± 1.1
+ MCFT	78.36±0.5	82.45±1.0	86.83±1.3	61.10±0.9	67.98±1.2	77.45±1.1

parameters. The EMA mechanism ensures stable updates by gradually incorporating changes, preventing abrupt shifts in the model’s behaviour. The final loss function combines the alignment and classification losses as: $\mathcal{L} = \mathcal{L}_{\text{align}} + \lambda \cdot \mathcal{L}_{\text{sup}}$, where λ is a weighting factor that balances the alignment and classification objectives.

Building on the core MCFT framework, we further propose a semi-supervised variant of MCFT, that leverages unlabelled data along with the limited labelled data to improve the performance. Let $X_{lb} = \{(x_i, y_i)_{i=1}^n\}$ and $X_{ulb} = \{(x_i)_{i=1}^N\}$ represent the labelled and unlabelled datasets, with $n \ll N$. The learning objective minimizes both supervised loss \mathcal{L}_{sup} and unsupervised loss \mathcal{L}_{unsup} as:

$$\min_{\theta} \left[\sum_{(x_i, y_i) \in X_{lb}} \mathcal{L}_{sup}(x_i, y_i, \theta) + \omega \sum_{x_i \in X_{ulb}} \mathcal{L}_{unsup}(x_i, \theta) \right], \quad (3)$$

$$\mathcal{L}_{em} = \frac{1}{\mu_B} \sum_{\theta=1}^{\mu_B} \mathbb{1} \left(\max(p_m(p_z(x_w^{(i)}))) \geq \tau \right) \cdot H \left(\arg \max(p_m(p_z(x_w^{(i)}))), p_m(p_z(x_s^{(i)})) \right), \quad (4)$$

For unsupervised learning, we adopt the concept of entropy minimization by using pseudo-labelling, where high-confidence predictions from weakly augmented samples serve as supervision for their strongly augmented counterparts. Inspired by Fix-Match [26], the unsupervised loss is defined in Eq. 4.

where τ is the confidence threshold, μ represents the ratio of unlabelled to labelled batch sizes, and H denotes the cross-entropy loss. To address the limitations of static thresholds and ensure the inclusion of all unlabelled samples, we adopt the semi-supervised framework from AllMatch ($\mathcal{L}_{AllMatch}$) [20]. This framework comprises

Table 2: Performance on ModelNet40 [40] in *n-way* few-shot setup.

Methods	5-way		10-way	
	10-shot	20-shot	10-shot	20-shot
OcCo [29]	94.0±3.6	95.9±2.3	89.4±5.1	92.4±4.6
Point-BERT [33]	94.6±3.1	96.3±2.7	91.0±5.4	92.7±5.1
MaskPoint [46]	95.0±3.7	97.2±1.7	91.4±4.0	93.4±3.5
Point-MAE [19]	96.3±2.5	97.8±1.8	92.6±4.1	95.0±3.0
Point-M2AE [41]	96.8±1.8	98.3±1.4	92.3±4.5	95.0±3.0
ACT [5]	96.8±2.3	98.0±1.4	93.3±4.0	95.6±2.8
RECON [22]	97.3±1.9	98.9±3.9	93.3±3.9	95.8±3.0
Point-BERT [33]	94.6±3.1	96.3±2.7	91.0±5.4	92.7±5.1
+ IDPT [35]	96.0± 1.7	97.2±2.6	91.9±4.4	93.6±3.5
+ DAPT [45]	95.8±2.1	97.3±1.3	92.2±4.3	94.2±3.4
+ PointGST [16]	96.5±2.4	97.9±2.0	92.7±4.2	95.0±2.8
+ MCFT	96.5±1.9	97.6±1.1	93.5±2.9	95.0±1.7
Point-MAE [19]	96.3±2.5	97.8±1.8	92.6±4.1	95.0±3.0
+ IDPT [35]	97.3±2.1	97.9±1.1	92.8±4.1	95.4± 2.9
+ DAPT [45]	96.8±1.8	98.0±1.0	93.0±3.5	95.5±3.2
+ PointGST [16]	98.0±1.8	98.3±0.9	93.7±4.0	95.7±2.4
+ MCFT	98.1±1.0	98.3±1.2	94.3±2.2	95.9±2.9

three modules: adaptive hard augmentation, inverse learning, and contrastive learning, which collectively enhance the use of unlabelled data to improve generalization, particularly when labelled data is limited. Finally, our unsupervised learning is the combination of the entropy minimization loss and alignment loss:

$$\mathcal{L}_{\text{unsup}} = \mathcal{L}_{\text{align}} + \mathcal{L}_{\text{EntMatch}} \quad (5)$$

To further enhance MCFT’s efficiency, we utilize a pruning technique that employs a salience scoring function to learn pruning masks [42]. This pruned version of MCFT improves the computational efficiency of transformer-based models for 3D point cloud processing, utilizing a pruning technique that employs a salience scoring function to learn pruning masks [42]. These masks identify and remove irrelevant blocks of model parameters, thereby reducing computational overhead during inference.

Let Θ denote the set of parameters of the transformer model, which consists of N layers. We define a pruning mask $m \in \{0, 1\}^N$, where $m_i = 1$ indicates that layer i is retained and $m_i = 0$ indicates that it is pruned. The salience score for each layer i is computed based on the gradient of the loss L with respect to the output E_i :

$$s_i = \frac{\partial L}{\partial E_i} \quad (6)$$

To obtain the salience score, we first calculate the mean and standard deviation of the salience scores across layers:

$$\mu_s = \frac{1}{N} \sum_{j=1}^N s_j, \quad \sigma_s = \sqrt{\frac{1}{N} \sum_{j=1}^N (s_j - \mu_s)^2} \quad (7)$$

The final salience score for each layer is normalized as:

$$\tilde{s}_i = \frac{s_i - \mu_s}{\sigma_s + \epsilon} \quad (8)$$

where ϵ is a small constant to prevent division by zero. Next, we mask the desired number of layers based on our pruning budget. The pruning process is iteratively applied every K epoch during fine-tuning, allowing the model to adapt to the changes in layer importance until we reach our desired pruning budget. Specifically, after every K epoch, the salience scores are recalculated, and the pruning mask is updated accordingly.

Table 3: Performance comparison of object recognition task in *fully-supervised* setting.

Method	#TP (M)	FLOPs	ScanObjectNN			ModelNet40
			BG	ONLY	PB	OA (%)
PointNet [43]	3.5	0.5	73.3	79.2	68.0	89.2
PointNet++ [21]	1.5	1.7	82.3	84.3	77.9	90.7
DGCNN [30]	1.8	2.4	82.8	86.2	78.1	92.9
PointMLP [18]	13.2	31.4	-	-	85.4	94.5
OcCo [29]	22.1	4.8	84.9	85.5	78.8	92.1
Point-BERT [33]	22.1	4.8	87.4	88.1	83.07	93.2
MaskPoint [46]	22.1	-	89.7	89.3	84.6	93.8
Point-MAE [19]	22.1	4.8	90.0	88.3	85.2	93.8
Point-M2AE [41]	15.3	3.6	91.2	88.8	86.4	94.0
ACT [5]	22.1	4.8	93.3	91.9	88.2	93.7
RECON [22]	43.6	5.3	94.2	93.1	89.7	93.9
Point-BERT [33]	22.1	4.8	87.4	88.1	83.1	93.2
+ PointPEFT [27]	22.8	-	-	-	85.0	-
+ IDPT [35]	23.8	7.2	88.1	88.3	83.7	93.4
+ DAPT [45]	23.2	5.0	91.1	89.7	85.4	93.6
+ PointGST [16]	22.7	4.8	91.4	89.7	85.6	93.8
+ MCFT	22.7	4.8	92.1	91.5	88.3	95.2
Point-MAE [19]	22.1	4.8	90.0	88.3	85.2	93.8
+ PPT [38]	23.4	4.8	92.9	92.4	88.4	93.4
+ MCST [6]	23.4	4.8	-	-	91.9	-
+ IDPT [35]	23.8	7.2	91.2	90.0	84.9	94.4
+ DAPT [45]	23.2	5.0	90.9	90.2	85.1	94.0
+ PointGST [16]	22.7	4.8	91.7	90.2	85.3	94.0
+ MCFT	22.7	4.8	91.8	90.9	87.2	94.9
RECON [22]	22.1	4.8	94.3	92.8	90.0	93.0
+ PPT [38]	23.2	-	94.1	93.2	88.9	93.4
+ MCST [6]	23.4	4.8	-	-	92.8	94.7
+ IDPT [35]	23.8	7.2	93.3	91.6	87.3	93.5
+ DAPT [45]	23.2	5.0	94.3	92.4	89.4	94.1
+ PointGST [16]	22.7	4.8	94.5	92.9	89.5	94.1
+ MCFT	22.7	4.8	94.9	93.1	90.8	95.2

Table 4: Performance of different PEFT methods.

Method	PB_T50_RS
Point-MAE [19]	85.18
Linear probing	75.99
+ Adapter [8]	83.93
+ Prefix tuning [13]	77.72
+ BitFit [34]	82.62
+ LoRA [9]	81.74
+ VPT-Deep [10]	81.09
+ AdaptFormer [2]	83.45
+ SSF [15]	82.58
+ IDPT [35]	84.94
+ DAPT [45]	85.08
+ PointGST [16]	85.29
+ MCFT	87.21

4 Experiments

Few-shot learning. In the full-few-shot setup, we evaluate MCFT on 5-, 10-, and 20-shot scenarios on both the ModelNet40 and ScanObjectNN datasets (Table 1), using PointMAE and PointBERT pre-trained encoders. For a fair comparison, we reproduce the performance of existing SOTA methods under identical experimental setups. Our experiments show that MCFT consistently outperforms the existing SOTAs across all few-shot scenarios. The largest improvement of *3.30%* is obtained in the 5-shot setting, where data is most limited. A similar result is also seen in 10- and 20-shot settings with the PointMAE encoder. With the PointBERT encoder, MCFT continues to outperform SOTA by a significant margin in all few-shot settings. A similar trend is also observed on the ScanObjectNN dataset.

We conduct an additional few-shot analysis following the conventional n -way m -shot setup commonly used in previous works [35, 45, 16]. Table 2 compares our method with existing approaches on 5-way 10-shot, 5-way 20-shot, 10-way 10-shot, and 10-way 20-shot settings on the ModelNet40 dataset. These settings represent relatively simpler few-shot tasks, where specific subsets of classes are selected for training. Even in these near-saturation conditions, MCFT outperforms SOTA, reinforcing its effectiveness within the few-shot learning paradigm.

Fully-supervised learning. In Table 3, we evaluate our proposed method on ModelNet40 and three variants of the ScanObjectNN dataset — OBJ_BG, OBJ_ONLY, and PB_T50_RS, each with distinct levels of complexity, following the evaluation protocol of most existing methods. For a fair comparison, we follow the reported results of existing methods, with Point-BERT, Point-MAE, and RECON as pre-trained models, as provided by [16]. As we observe from Table 3, MCFT outperforms existing SOTA by 0.7%, 1.8%, and 2.7% on the three variants of ScanObjectNN with Point-BERT encoder, while having similar FLOPs and total parameters to the pre-trained encoder. Similar trends are observed with Point-MAE and RECON as a backbone, underscoring the efficiency of MCFT. On the ModelNet40 dataset, though the performance of existing models is near saturation, our method still demonstrates consistent performance gain over SOTA methods, with a 1.4% improvement for the Point-BERT encoder.

In Table 4, we compare MCFT with several existing PEFT techniques originally developed for NLP and vision tasks. These results, also adopted from [45], were performed on the PB_T50_RS variant of ScanObjectNN, the most challenging variant. PointMAE is used as the pre-trained encoder for this experiment. While most of the existing PEFT methods typically introduce additional parameters during training, increasing compu-

Table 5: Performance on part segmentation task on ShapeNetPart.

Methods	mIoU	
	Cls.	Inst.
PointNet [43]	80.4	83.7
PointNet++ [21]	81.9	85.1
DGCNN [30]	82.3	85.2
MaskPoint [46]	84.6	86.0
Point-BERT [33]	84.1	85.6
Point-MAE [19]	84.2	86.1
ACT [5]	84.7	86.1
Point-BERT [33]	84.1	85.6
+ IDPT [35]	83.5	85.3
+ PointPEFT [27]	81.1	84.3
+ DAPT [45]	83.8	85.5
+ PointGST [16]	83.9	85.7
+ MCFT	85.2	87.1
Point-MAE [19]	84.2	86.1
+ IDPT [35]	83.8	85.7
+ PointPEFT [27]	83.2	85.2
+ DAPT [45]	84.0	85.7
+ PointGST [16]	83.8	85.8
+ MCFT	86.4	89.0
ReCon [22]	84.5	86.1
+ IDPT [35]	83.7	85.7
+ PointPEFT [27]	83.1	85.1
+ DAPT [45]	83.9	85.7
+ PointGST [16]	84.0	85.8
+ MCFT	84.4	86.8

tational overhead during inference, MCFT outperforms all the existing PEFT methods with substantial margins without introducing additional parameters.

Part segmentation. To assess MCFT’s performance in a dense prediction task, we evaluate it on the more challenging problem of part segmentation, where the goal is to predict a semantic label for each point in a 3D shape. Following prior work [45], we benchmark MCFT on the ShapeNetPart dataset [32]. As shown in Table 5, MCFT surpasses SOTA methods by a significant 2.6 and 3.2 mIoU in both class-level and instance-level.

Semi-supervised approach. Table 6 compares the semi-supervised variant of our proposed method against state-of-the-art methods on the ModelNet40 dataset in the 5-shot setting (*full few-shot*). Here, only a small portion of labelled data (5 samples per class) is available, along with the remaining data as the unlabelled set. We report the average accuracy as well as the standard deviation over 3 runs. The semi-supervised variant of MCFT shows significant improvement (84.49%) over the fully-supervised variant and improved existing SOTA by 9.43%, showing the positive impact of utilizing unlabelled data in tuning a foundation model under few-shot setup.

In Table 7, we further compare the performance of MCFT(SSL) with different semi-supervised methods from various domains on the ModelNet40 dataset. For a fair comparison, we reproduce the performance of different SSL methods under the 5-shot setting with the PointMAE encoder and report the overall accuracy. Here, MCFT continues to gain a substantial improvement over all methods.

Pruning approach. As discussed in the method section, structural pruning selectively removes less significant encoder layers to improve computational efficiency. Table 8 shows the effect of pruning on the semi-supervised MCFT variant under the 5-shot setup. The compressed MCFT outperforms existing SOTA methods by 8.45%. Additionally, it surpasses our supervised variant by 5.15% with 1.8M fewer parameters in total. This light-weight version of MCFT maintains strong performance while reducing computational overhead, making it well-suited for resource-constrained applications.

Inference Time Analysis. Table 9 compares different fine-tuning methods for 3D foundation models based on trainable parameters, computational cost (FLOPs), processing efficiency (throughput), and performance (PB_T50_RS). MCFT achieves the highest performance (87.2%) while maintaining efficiency,

Table 6: Performance on semi-supervised setting on ModelNet40.

Methods	5-shot
Point-MAE [19]	73.32±2.1
+ IDPT [35]	73.51 ±2.8
+ DAPT [45]	73.74±1.6
+ PointGST [16]	75.06±1.9
+ MCFT	78.36±0.5
+ MCFT (SSL)	84.49±0.7

Table 7: Comparison of different SSL approaches.

Method	Accuracy
Point-MAE [19]	73.32
Linear probing	71.09
+ FixMatch [26]	73.48
+ FlexMatch [36]	75.51
+ Dash [31]	74.81
+ Chen <i>et al.</i> [1]	74.37
+ M2CP [3]	79.88
+ Confid [4]	81.24
+ AllMatch [20]	82.62
+ MCFT w. AllMatch	84.49

Table 8: Performance of the pruned variant of MCFT under semi-supervised setting.

Methods	# TP (M)	5-shot
Point-MAE [19]	22.1	73.32±2.1
+ IDPT [35]	23.8	73.51 ±2.8
+ DAPT [45]	23.2	73.74±1.6
+ PointGST [16]	22.7	75.06±1.9
+ MCFT	22.7	78.36±0.5
+ MCFT (SSL)	22.7	84.49±0.7
+ MCFT (pruned)	20.9	83.51±1.1

with 22.7M parameters and 4.8G FLOPs, comparable to Point-MAE but outperforming it. MCFT (pruned) further reduces parameters (20.9M) and FLOPs (4.4G), significantly improving throughput (350.75 frames/s) but with a slight performance drop (83.5%), making it ideal for resource-constrained scenarios.

Sensitivity study. We conduct a comprehensive sensitivity analysis on MCFT using ModelNet40 to evaluate the impact of key hyperparameters. The EMA value plays a critical role in balancing adaptation and stability, with EMA = 0.999 achieving the best performance, while lower values risk overfitting and higher values limit learning.

Pruning analysis shows that removing one encoder layer incurs only a minor accuracy drop, whereas aggressive or excessive pruning leads to sharp degradation, highlighting the importance of gradual pruning. The pruning schedule is also influential, where pruning one layer every $K = 10$ epochs yields the best accuracy and stability compared to more frequent or delayed schedules. Additionally, the model is relatively robust to variations in the loss factor, achieving optimal performance at a value of 1.0. Finally, delaying full fine-tuning beyond 50 epochs negatively impacts accuracy, indicating that an early transition to full fine-tuning is crucial for optimal performance.

Table 9: Comparison of inference efficiency on object recognition task on ScanObjectNN. We measure throughput with a batch size of 32 on a single RTX 4090 GPU.

Method	#TP(M)	FLOPs(G)	Throughput (frame/s)	PB_T50_RS
Point-MAE [19]	22.1	4.8	323.66	85.2
IDPT [35]	23.8	7.2	281.18	84.9
DAPT [45]	23.2	5.0	311.28	85.1
+ MCFT	22.7	4.8	321.58	87.2
+ MCFT (pruned)	20.9	4.4	350.75	83.5

5 Conclusion

We introduced Momentum-Consistency Fine-Tuning (MCFT), an adapter-free approach for adapting 3D foundation models in data-scarce settings. By selectively fine-tuning the encoder while enforcing momentum-based consistency, MCFT effectively mitigates overfitting and representation drift commonly observed in full fine-tuning, without incurring the inference-time overhead of PEFT methods. This positions MCFT as a practical middle ground between full and parameter-efficient fine-tuning. Extensive evaluations on object recognition and part segmentation tasks show that MCFT consistently outperforms existing approaches across few-shot, full few-shot, and fully supervised setups, achieving a notable 3.30% improvement in the 5-shot regime. We further demonstrate that leveraging unlabeled data through a semi-supervised extension yields additional performance gains, while a structured pruning variant maintains comparable accuracy with reduced computational cost, making MCFT suitable for deployment on resource-constrained devices. While MCFT is effective, its performance depends on the choice of momentum and pruning hyperparameters, which may require dataset-specific tuning. Future work will explore adaptive strategies for hyperparameter selection and extend MCFT to more complex 3D understanding tasks, including large-scale scene-level reasoning.

References

1. Chen, L., Zhang, Y., Lin, Y., Jiang, M., Huang, Y., Lei, Y.: Consistency-based semi-supervised learning for point cloud classification. In: 2021 4th International Conference on Pattern Recognition and Artificial Intelligence (PRAI). pp. 440–445. IEEE (2021)
2. Chen, S., Ge, C., Tong, Z., Wang, J., Song, Y., Wang, J., Luo, P.: Adaptformer: Adapting vision transformers for scalable visual recognition. *Advances in Neural Information Processing Systems* **35**, 16664–16678 (2022)
3. Chen, Z., Jing, L.: Multimodal semi-supervised learning for 3d objects. In: The British Machine Vision Conference (BMVC) (2021)
4. Chen, Z., Jing, L., Yang, L., Li, Y., Li, B.: Class-level confidence based 3d semi-supervised learning. In: Proceedings of the IEEE/CVF Winter Conference on Applications of Computer Vision. pp. 633–642 (2023)
5. Dong, R., Qi, Z., Zhang, L., Zhang, J., Sun, J., Ge, Z., Yi, L., Ma, K.: Autoencoders as cross-modal teachers: Can pretrained 2d image transformers help 3d representation learning? In: The Eleventh International Conference on Learning Representations
6. Han, X., Tang, Y., Xu, J., Li, X.: Most: Efficient monarch sparse tuning for 3d representation learning. In: Proceedings of the Computer Vision and Pattern Recognition Conference. pp. 6584–6594 (2025)
7. Hedegaard, L., Alok, A., Jose, J., Iosifidis, A.: Structured pruning adapters. *Pattern Recognition* **156**, 110724 (2024)
8. Houshy, N., Giurgiu, A., Jastrzebski, S., Morrone, B., De Laroussilhe, Q., Gesmundo, A., Attariyan, M., Gelly, S.: Parameter-efficient transfer learning for nlp. In: International conference on machine learning. pp. 2790–2799. PMLR (2019)
9. Hu, E.J., Wallis, P., Allen-Zhu, Z., Li, Y., Wang, S., Wang, L., Chen, W., et al.: Lora: Low-rank adaptation of large language models. In: International Conference on Learning Representations
10. Jia, M., Tang, L., Chen, B.C., Cardie, C., Belongie, S., Hariharan, B., Lim, S.N.: Visual prompt tuning. In: European Conference on Computer Vision. pp. 709–727. Springer (2022)
11. Lagunas, F., Charlaix, E., Sanh, V., Rush, A.M.: Block pruning for faster transformers. In: Proceedings of the 2021 Conference on Empirical Methods in Natural Language Processing. pp. 10619–10629 (2021)
12. Lester, B., Al-Rfou, R., Constant, N.: The power of scale for parameter-efficient prompt tuning. In: Proceedings of the 2021 Conference on Empirical Methods in Natural Language Processing. Association for Computational Linguistics (2021)
13. Li, X.L., Liang, P.: Prefix-tuning: Optimizing continuous prompts for generation. In: Proceedings of the 59th Annual Meeting of the Association for Computational Linguistics and the 11th International Joint Conference on Natural Language Processing (Volume 1: Long Papers). Association for Computational Linguistics (2021)
14. Li, Y., Luo, F., Tan, C., Wang, M., Huang, S., Li, S., Bai, J.: Parameter-efficient sparsity for large language models fine-tuning. *International Joint Conferences on Artificial Intelligence* (2022)
15. Lian, D., Zhou, D., Feng, J., Wang, X.: Scaling & shifting your features: A new baseline for efficient model tuning. *Advances in Neural Information Processing Systems* **35**, 109–123 (2022)
16. Liang, D., Feng, T., Zhou, X., Zhang, Y., Zou, Z., Bai, X.: Parameter-efficient fine-tuning in spectral domain for point cloud learning. *IEEE Transactions on Pattern Analysis and Machine Intelligence* (2025)

17. Luo, G., Huang, M., Zhou, Y., Sun, X., Jiang, G., Wang, Z., Ji, R.: Towards efficient visual adaption via structural reparameterization. arXiv preprint arXiv:2302.08106 (2023)
18. Ma, X., Qin, C., You, H., Ran, H., Fu, Y.: Rethinking network design and local geometry in point cloud: A simple residual mlp framework. In: International Conference on Learning Representations
19. Pang, Y., Wang, W., Tay, F.E., Liu, W., Tian, Y., Yuan, L.: Masked autoencoders for point cloud self-supervised learning. In: European conference on computer vision. pp. 604–621. Springer (2022)
20. Paul, S., Patterson, Z., Bouguila, N.: Improving 3d semi-supervised learning by effectively utilizing all unlabelled data. In: European Conference on Computer Vision. pp. 55–71. Springer (2024)
21. Qi, C.R., Yi, L., Su, H., Guibas, L.J.: Pointnet++: Deep hierarchical feature learning on point sets in a metric space. *Advances in neural information processing systems* **30** (2017)
22. Qi, Z., Dong, R., Fan, G., Ge, Z., Zhang, X., Ma, K., Yi, L.: Contrast with reconstruct: Contrastive 3d representation learning guided by generative pretraining. In: International Conference on Machine Learning. pp. 28223–28243. PMLR (2023)
23. Roy, S., Etemad, A.: Consistency-guided prompt learning for vision-language models. In: International Conference on Learning Representations (2024)
24. Ruan, J., Gao, J., Xie, M., Xiang, S., Pan, C.: Gist: Improving parameter efficient fine-tuning via knowledge interaction. In: Proceedings of the 32nd ACM International Conference on Multimedia. pp. 8835–8844 (2024)
25. Sanh, V., Wolf, T., Rush, A.: Movement pruning: Adaptive sparsity by fine-tuning. *Advances in neural information processing systems* **33**, 20378–20389 (2020)
26. Sohn, K., Berthelot, D., Carlini, N., Zhang, Z., Zhang, H., Raffel, C.A., Cubuk, E.D., Kurakin, A., Li, C.L.: Fixmatch: Simplifying semi-supervised learning with consistency and confidence. *Advances in neural information processing systems* **33**, 596–608 (2020)
27. Tang, Y., Zhang, R., Guo, Z., Ma, X., Zhao, B., Wang, Z., Wang, D., Li, X.: Pointpeft: Parameter-efficient fine-tuning for 3d pre-trained models. In: Proceedings of the AAAI Conference on Artificial Intelligence. vol. 38, pp. 5171–5179 (2024)
28. Uy, M.A., Pham, Q.H., Hua, B.S., Nguyen, T., Yeung, S.K.: Revisiting point cloud classification: A new benchmark dataset and classification model on real-world data. In: International Conference on computer vision. pp. 1588–1597 (2019)
29. Wang, H., Liu, Q., Yue, X., Lasenby, J., Kusner, M.J.: Unsupervised point cloud pre-training via occlusion completion. In: International Conference on computer vision. pp. 9782–9792 (2021)
30. Wang, Y., Sun, Y., Liu, Z., Sarma, S.E., Bronstein, M.M., Solomon, J.M.: Dynamic graph cnn for learning on point clouds. *ACM Transactions on Graphics (tog)* **38**(5), 1–12 (2019)
31. Xu, Y., Shang, L., Ye, J., Qian, Q., Li, Y.F., Sun, B., Li, H., Jin, R.: Dash: Semi-supervised learning with dynamic thresholding. In: International conference on machine learning. pp. 11525–11536 (2021)
32. Yi, L., Kim, V.G., Ceylan, D., Shen, I.C., Yan, M., Su, H., Lu, C., Huang, Q., Sheffer, A., Guibas, L.: A scalable active framework for region annotation in 3d shape collections. *ACM Transactions on Graphics (ToG)* **35**(6), 1–12 (2016)
33. Yu, X., Tang, L., Rao, Y., Huang, T., Zhou, J., Lu, J.: Point-bert: Pre-training 3d point cloud transformers with masked point modeling. In: Proceedings of the IEEE/CVF conference on computer vision and pattern recognition. pp. 19313–19322 (2022)

34. Zaken, E.B., Goldberg, Y., Ravfogel, S.: Bitfit: Simple parameter-efficient fine-tuning for transformer-based masked language-models. In: Proceedings of the 60th Annual Meeting of the Association for Computational Linguistics (Volume 2: Short Papers). pp. 1–9 (2022)
35. Zha, Y., Wang, J., Dai, T., Chen, B., Wang, Z., Xia, S.T.: Instance-aware dynamic prompt tuning for pre-trained point cloud models. In: Proceedings of the IEEE/CVF International Conference on Computer Vision. pp. 14161–14170 (2023)
36. Zhang, B., Wang, Y., Hou, W., Wu, H., Wang, J., Okumura, M., Shinozaki, T.: Flexmatch: Boosting semi-supervised learning with curriculum pseudo labeling. *Advances in Neural Information Processing Systems* **34**, 18408–18419 (2021)
37. Zhang, M., Chen, H., Shen, C., Yang, Z., Ou, L., Yu, X., Zhuang, B.: Loraprune: Structured pruning meets low-rank parameter-efficient fine-tuning. In: Findings of the Association for Computational Linguistics: ACL 2024. pp. 3013–3026 (2024)
38. Zhang, S., Qi, Z., Dong, R., Bai, X., Wei, X.: Positional prompt tuning for efficient 3d representation learning. In: Proceedings of the 33rd ACM International Conference on Multimedia. pp. 1171–1180 (2025)
39. Zhang, X., Li, Y., Zhang, X.: Boosting few-shot point cloud segmentation with intra-class correlation and iterative prototype fusion. *Computer Vision and Image Understanding* p. 104393 (2025)
40. Zhang, X., Sugano, Y., Fritz, M., Bulling, A.: Appearance-based gaze estimation in the wild. In: Proceedings of the IEEE conference on computer vision and pattern recognition. pp. 4511–4520 (2015)
41. Zhang, Y., Lin, J., Li, R., Jia, K., Zhang, L.: Point-ma2e: Masked and affine transformed autoencoder for self-supervised point cloud learning. *arXiv preprint arXiv:2211.06841* (2022)
42. Zhao, B., Hajishirzi, H., Cao, Q.: Apt: adaptive pruning and tuning pretrained language models for efficient training and inference. In: Proceedings of the 41st International Conference on Machine Learning. pp. 60812–60831 (2024)
43. Zhao, H., Shi, J., Qi, X., Wang, X., Jia, J.: Pyramid scene parsing network. In: Proceedings of the IEEE conference on computer vision and pattern recognition. pp. 2881–2890 (2017)
44. Zhao, W., Huang, Y., Han, X., Liu, Z., Zhang, Z., Sun, M.: Cpet: Effective parameter-efficient tuning for compressed large language models. *arXiv preprint arXiv:2307.07705* (2023)
45. Zhou, X., Liang, D., Xu, W., Zhu, X., Xu, Y., Zou, Z., Bai, X.: Dynamic adapter meets prompt tuning: Parameter-efficient transfer learning for point cloud analysis. In: Proceedings of the IEEE/CVF conference on computer vision and pattern recognition (2024)
46. Zhuang, W., Chu, Q., Tan, Z., Liu, Q., Yuan, H., Miao, C., Luo, Z., Yu, N.: Uia-vit: Unsupervised inconsistency-aware method based on vision transformer for face forgery detection. In: European conference on computer vision. pp. 391–407. Springer (2022)